ELSEVIER

Journal of Hazardous Materials A103 (2003) 217–229

Journal of Hazardous Materials

www.elsevier.com/locate/jhazmat

Shallow layer simulation of heavy gas released on a slope in a calm ambient Part II. Instantaneous releases

Robin K.S. Hankin*

School of Geography and Environmental Science, The University of Auckland, Private Bag 92019, Glen Innes, Auckland, New Zealand

Received 24 February 2003; received in revised form 4 July 2003; accepted 8 July 2003

Abstract

This paper assesses the value of shallow layer modelling for instantaneous releases of heavy gas over a slope using the established computer model TWODEE [R.K.S. Hankin, Heavy gas dispersion over complex terrain, Ph.D. thesis, Cambridge University, 1997; J. Hazard. Mater. 66 (1999) 211; J. Hazard. Mater. 66 (1999) 227; J. Hazard. Mater. 66 (1999) 239] and the experimental results of Schatzmann et al. [M. Schatzmann, K. Marotzke, J. Donat, Research on continuous and instantaneous heavy gas clouds, Contribution of sub-project EV 4T-0021-D to the final report of the joint CEC project, Technical report, Meteorological Institute, University of Hamburg, February 1991].

This is the second of a two-part paper; part I considered continuous releases using the same model, using the same entrainment parameters. Schatzmann et al. carried out instantaneous releases of heavy gas over three slopes; each experiment was repeated five times under nominally identical conditions.

The goodness-of-fit measures (GFMs) of Hanna et al. [Atmos. Environ. 27A (15) (1993) 2265] are generalized to account for the multiple releases carried out by Schatzmann et al. Using these statistical GFMs, predicted peak concentrations are generally correct to within a factor of two; and cloud arrival times are generally late.

Keywords: Heavy gas dispersion; Instantaneous releases; Shallow layer modelling; Risk assessment; Slopes

1. Introduction

Part I of this two-part paper assessed the value of shallow layer modelling for continuous releases using the established computer model TWODEE [1–4] and the experimental

* Tel.: +64-9-373-7599; fax: +64-9-373-7042.
E-mail address: r.hankin@auckland.ac.nz (R.K.S. Hankin).

0304-3894/$ – see front matter © 2003 Elsevier B.V. All rights reserved.
doi:10.1016/S0304-3894(03)00225-5

results of Schatzmann et al. [5]; this part considers instantaneous releases using the same methodology and model.

In the field of major hazard (chlorine) risk assessment, instantaneous releases are typically considered to have a failure rate of 2×10^{-6} Pa—compare continuous releases at 40×10^{-6} Pa—and are thus rarer than continuous releases but are usually considered to be of greater mortality [7].

From a physical perspective, instantaneous releases are considerably more complex than continuous releases because an instantaneous release is inherently time-varying, while a continuous release may be viewed as a steady-state system.

Experimental data for instantaneous releases are typically of the form of a large number of Eulerian concentration traces, measured by sensors located at fixed positions [8]. Field experiments especially may result in many tens of traces, each of which is a time-series that may consist of over 1000 measurements.

It is often unclear how such large datasets may be compared with model results. In this paper, I suggest a method by which an experimental dataset may be compared with output from a shallow layer model; validation techniques typically used for integral models are not necessarily appropriate because of the very different representations used for the cloud [9].

Although this paper focuses on industrial risk assessment and heavy gas dispersion, shallow layer models are more widely applicable. Simpson [10] considered buoyancy driven flow on slopes in the context of powder snow avalanches, nuees ardentes, oceanic turbidity currents, and heavy gas dispersion. Here, attention will be confined to buoyancy conserving flows.

1.1. Modelling instantaneous releases

Although shallow layer modelling is a natural approach to dense gas dispersion, other methods do exist including CFD and integral models; the CFD approach was discussed in part I.

Tickle [11], building on the work of Webber and Wren [12], presented a model of the motion of an instantaneously released heavy gas cloud released on a uniform slope. A wedge-shaped cloud was demonstrated to be a solution to the resisted shallow water equations on a slope, although the boundary conditions were different from those used here (Eq. (1) of part I).

Tickle's model had two empirically determined constants; this would mean that the GFMs discussed in Section 3.1.1 would not be appropriate.

2. The instantaneous release experiments of Schatzmann et al. [5]

Schatzmann et al. [5] released either 125 or 450 cm^3 of SF_6 from a cylinder of aspect ratio of approximately unity over each of three slopes (4.0, 8.6, and 11.63%). The release mechanism was a scaled version of that used in the Thorney Island Trials [13]; a small cylinder was filled with dense gas and the side walls were abruptly retracted into the tunnel floor [5,12,14]. Sensors were artificially aspirated hot-wire anemometers with a sampling rate of either 10 or 12.5 Hz—compare the shallow layer frequency $\sqrt{g'/h} \simeq 4$ Hz at cloud arrival time.

Each experiment was repeated five times under nominally identical conditions and concentration traces from each of eight sensors were recorded. There are thus $3 \times 5 \times 8 = 120$ traces. Each trace continued for 70 or 80 s [15].

3. Statistics for instantaneous releases

The typical traces for an instantaneous release shown in Fig. 1 suggest several statistics that may be useful for model evaluation.

Cloud arrival time is defined as the first time for which the cloud concentration exceeds half the peak value.

Cloud residence time should reflect the length of time for which the concentration remains appreciably greater than background levels. The cloud residence time clearly requires objective definition, but its determination can be difficult as the concentration tends to decrease very slowly after an initial sharp rise.

Here, a cloud departure time t_d is defined as the last time at which the cloud concentration exceeds half its maximum value. Although this time is usually well-defined, some traces exhibit slowly-decaying concentrations around $t = t_d$. Cloud residence time t_r is defined as $t_r = t_d - t_a$.

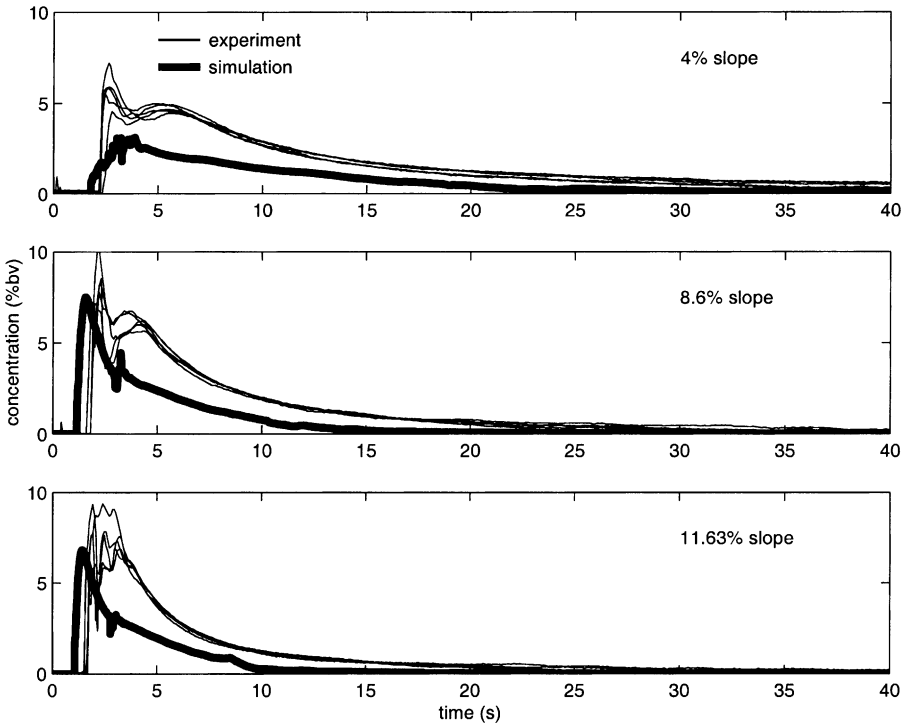

Fig. 1. Eulerian concentration traces at (61, 0) for each slope. From top to bottom: 4, 8.6, and 11.63%.

Peak concentration is clearly defined as the maximal concentration experienced at a given sensor. Peak concentration is the only quantity used for calculation of GFMs (for instantaneous dense releases) by Hanna et al. [6]. It is convenient, unambiguous, and important in risk assessment. An incorrect prediction of peak concentration usually has a clear interpretation when considering a model.

3.1. GFMs for instantaneous releases

Because the instantaneous releases were repeated, Hanna et al.'s GFMs are not appropriate. Instead, a formal assessment based on observations of Davies [16] will be used, and a slight modification of Hanna et al.'s FAC2 will be used. For cloud arrival times, the proportion FIN of predicted times between the latest and earliest cloud arrival times will be used: under H_0, the expectation of FIN would be $2/3$.

3.1.1. Formal assessment

An appropriate goodness-of-fit criterion was given by Davies [16]:

$$\phi = \sum_{i=1}^{N} \left(\frac{\ln(C_{\mathrm{o},i}) - \ln(C_{\mathrm{p},i})}{\sigma_{\mathrm{o},i}} \right)^2 \tag{1}$$

where $1 \leq i \leq N$ is the number of observations and subscripts 'p' and 'o' stand for predicted and observed values. The denominator $\sigma_{\mathrm{o},i}$ is a weighting factor that accounts for ensemble variability. Davies discussed properties of ϕ for the case of equal $\sigma_{\mathrm{o},i}$. Hanna et al. [6] pointed out that Davies's arguments depend upon knowing the value of σ_{o}; in the present context, the repeated trials provide information about the variance due to inherent uncertainty [17]. There is no evidence to suggest that Davies's assumption of homoscedasticity is incorrect (the Fligner–Killeen test [18] is appropriate here, being "robust and powerful" when the population means are unknown [19]. It gives P-values of 0.4, 0.3, and 0.57, respectively), and thus following Davies's assumption of constant variance appears to be reasonable. If this is so, the appropriate statistics would be

$$\mathrm{tG} = \frac{U\sqrt{39}}{V\sqrt{40}} \sim t_{40}, \qquad \mathrm{FG} = \frac{5W/8}{X/32} \sim F_{8,32} \tag{2}$$

where

$$U = \sum_{\substack{i=1 \\ \text{sensor}}}^{8} \sum_{\substack{j=1 \\ \text{trial}}}^{5} \left(\ln(C_{\mathrm{o},i;j}) - \ln(C_{\mathrm{p},i}) \right) \tag{3}$$

$$V^2 = \sum_{\substack{i=1 \\ \text{sensor}}}^{8} \sum_{\substack{j=1 \\ \text{trial}}}^{5} \left(\ln(C_{\mathrm{o},i;j}) - \ln(C_{\mathrm{p},i}) - \frac{U}{40} \right)^2 \tag{4}$$

$$W = \sum_{\substack{i=1 \\ \text{sensor}}}^{8} (\overline{\ln(C_{\mathrm{o},i})} - \ln(C_{\mathrm{p},i}))^2 \tag{5}$$

$$X = \sum_{\substack{i=1 \\ \text{sensor}}}^{8} \sum_{\substack{j=1 \\ \text{trial}}}^{5} (\ln(C_{\mathrm{o},i;j}) - \overline{\ln(C_{\mathrm{o},i})})^2 \tag{6}$$

Thus, tG and FG correspond to MG and VG respectively, although neither is meaningful for a single observation. The 95% critical regions would be $|\mathrm{tG}| > 2.02$ (two-sided) and $\mathrm{FG} > 2.24$ (one-sided). The Bonferroni correction would give values of 2.50 and 2.84, respectively. This approach would have to be modified for Tickle's wedge-shaped model [11], as two free parameters were fitted to the experimental data.

3.1.2. Nonparametric GFMs

A slight modification of Hanna et al.'s nonparametric FAC2 (the fraction of predictions correct to within a factor of 2) is necessary to accommodate Schatzmann et al.'s multiple observations.

If $R = \ln(\overline{C_{\mathrm{o},i}}) - \ln(C_{\mathrm{p},i})$ is the mean log residual at the ith sensor, and H_x is the hypothesis that $R = x$, then the appropriate criterion would be whether there is *statistical* evidence to suggest that H_x is incorrect for all x with $|x| \leq \ln 2$. It is convenient to write H_{FAC2} for the composite hypothesis that H_x is true for some x with $|x| \leq \ln 2$. No exact method exists for H_{FAC2} because a prior for x is not available.

The likelihood approach of Edwards [20] is suitable for testing H_{FAC2}. An appropriate criterion would be that there exists an x with $|x| \leq \ln 2$ such that two units of likelihood would be lost (from H_{C_p}) by adopting H_x. If such an x exists, then this is strong evidence that H_{FAC2} is incorrect. Hanna et al.'s FAC2 then becomes the fraction of sensors for which H_{FAC2} is accepted (in this paradigm, failure to reject H_{FAC2} implies "accepting" it; the sense is that H_{FAC2} cannot readily be bettered [20]).

This approach is readily generalized to assess whether there is evidence to suggest the residual is either positive (H_+) or negative (H_-). Thus, $H_\pm$ may be tested according to the same criterion as above. Rejection would be evidence in favor of a positive or negative residual respectively; Table 1 summarizes a reasonable terminology for describing the residual. Thus "$\lesssim$" would mean that evidence exists to suggest the residual was negative,

Table 1
Symbols for use in Table 2 when comparing repeated observations with predictions

H_{FAC2}	H_+	H_-	Symbol
A	A	A	$\approx$
A	R	A	$\lesssim$
A	A	R	$\gtrsim$
R	R	A	$<$
R	A	R	$>$

but none to suggest that the residual were as low as $-\ln 2$ (implying $\overline{C_o}/C_p < 0.5$). Not all combinations are meaningful.

4. Results for instantaneous releases

4.1. Formal statistical results

Table 2 shows predicted and observed peak concentrations and Table 3 shows cloud arrival times.

The tG statistic is outside the critical region for the 4 and 8.6% slopes, but above it for the 11.63% slope (3.03 corresponds to a P-value of 0.64% if a Bonferroni correction is applied). Thus, there is no significant trend of over- or underprediction for the two flatter slopes, for the sensors as a whole. The 11.63% slope exhibits underprediction, significant at the 1% level, but not the 0.5% level.

The FG statistic is over the critical value of 2.24 for all three slopes, so there is convincing evidence to reject the null hypothesis that the mean observed concentrations are equal to the predicted concentration at each sensor. However, this is largely due to the small variance of observations, caused by Schatzmann et al.'s conducting their experiments in a calm ambient. Outdoors, atmospheric turbulence would increase σ_o and therefore increase the range of acceptable predictions.

Table 2
Coordinates, and observed and predicted peak concentrations for all eight sensors in each of Schatzmann et al.'s three instantaneous release experiments; measurements in cm, source at (0, 0)

Coordinates/slope (%)	Concentration (%): observed [minimum, maximum] vs. predicted		
	4	8.6	11.63
(61, 0)[a]	[4.7, 7.2] $\gtrsim$ 3.1	[6.6, 10.1] $\approx$ 7.5	[6.7, 9.4] $\gtrsim$ 6.8
(61, 23)	n/a	n/a	[6.2, 7.9] $\approx$ 7.2
(61, 46)	[1.9, 2.2] $\lesssim$ 2.4	[2.3, 2.6] $\gtrsim$ 1.5	[1.8, 2.4] $>$ 0.6
(61, 77)	[0.3, 0.7] $\lesssim$ 1.0	[0.3, 0.4] $\lesssim$ 0.5	n/a
(123, 0)[a]	[1.5, 1.8] $\gtrsim$ 1.0	[2.8, 3.5] $\gtrsim$ 1.4	[2.7, 4.0] $\gtrsim$ 2.1
(123, 23)	n/a	n/a	[2.6, 3.3] $\lesssim$ 4.9
(123, 38)	[0.8, 1.1] $\gtrsim$ 0.8	[1.5, 1.8] $\approx$ 1.7	[1.3, 1.6] $\lesssim$ 2.1
(123, 77)	[0.3, 0.5] $\lesssim$ 0.8	[0.3, 0.7] $\lesssim$ 1.0	n/a
(184, 0)[a]	[0.9, 1.1] $\gtrsim$ 0.6	[1.4, 1.7] $\gtrsim$ 1.0	[1.2, 1.8] $\gtrsim$ 0.9
(184, 38)	[0.5, 0.7] $\gtrsim$ 0.5	[0.7, 1.1] $\lesssim$ 1.5	[0.8, 1.1] $\gtrsim$ 0.5
GFMs: all sensors			
FAC2	1	1	0.875
tG	0.38	0.46	3.03
FG	54.7	59.6	103.1
GFMs: centreline sensors			
FAC2[a]	1	1	1
tG[a]	16.5	5.54	7.13
FG[a]	116	141	33.6

Symbols "$\approx$", "$\gtrsim$" and "$\lesssim$" are defined in Table 1.
[a] Denotes a centerline sensor.

Table 3
Coordinates, and observed and predicted cloud arrival times for all eight sensors in each of Schatzmann et al.'s three instantaneous release experiments; measurements in cm, source at (0, 0)

Coordinates/slope (%)	Arrival time (s): observed [minimum, maximum] vs. predicted		
	4	8.6	11.63
(61, 0)[a]	[2.3, 2.6] > 1.8	[1.4, 1.5] > 1.2	[1.6, 1.8] > 1.1
(61, 23)	n/a	n/a	[2.1, 2.3] < 5.2
(61, 46)	[4.0, 4.3] < 6.0	[2.6, 2.9] < 5.8	[2.8, 3.2] < 9.4
(61, 77)	[10.1, 11.6] ≈ 10.4	[7.4, 8.3] < 10.6	n/a
(123, 0)[a]	[10.0, 11.4] ≈ 10.1	[4.4, 4.9] < 6.7	[4.4, 5.2] < 5.7
(123, 23)	n/a	n/a	[4.6, 5.5] < 12.7
(123, 38)	[11.9, 13.4] ≈ 12.0	[5.6, 6.1] < 10.0	[5.6, 6.1] < 8.9
(123, 77)	[18.7, 21.4] < 16.9	[4.6, 6.5] < 15.0	n/a
(184, 0)[a]	[17.8, 20.1] < 20.5	[8.6, 9.6] < 15.5	[7.8, 9.0] < 12.6
(184, 38)	[21.5, 24.7] > 21.4	[9.4, 11.0] < 16.4	[9.4, 11.8] < 14.2
GFMs: all sensors			
FIN	0.38	0	0
GFMs: centreline sensors			
FIN[a]	0.33	0	0

Symbols "≈", "<" and ">" are defined in Table 1.
[a] Denotes a centerline sensor.

Atmospheric variability would decrease tG and FG by increasing V and X (Eqs. (4) and (6)); Wilson [21] suggests that in field trials, peak concentrations vary by a factor of 10 from trial to trial, under nominally identical conditions. If their logarithms were uniformly distributed over this range, the variance would be $\ln(10)^2/12 \simeq 0.44$. This is considerably greater than the variance observed in Schatzmann et al.'s experiments where the maximum likelihood estimate is about 0.1 for each slope.

The model predictions measured against the FAC2 criterion are more encouraging: H_{FAC2} is accepted for 23 of the 24 sensor/slope combinations. Thus, correct predictions to within a factor of two are generally observed.

Centreline sensors: The centreline sensors may be considered as a separate group. However, it should be noted that this is not equivalent to considering confined channel flow on a slope (such as considered by Ellison and Turner [22]) because lateral spread cannot be neglected for unconstrained flow.

Nevertheless, the centreline does offer insight into the model's overall behaviour and Tables 2 and 3 include the GFMs evaluated for the centreline sensors in isolation. Although the FAC2 score is slightly improved, the tG and FG statistics are all significant, in this case indicating underprediction.

4.1.1. Cloud arrival time

Table 3 shows that cloud arrival time is generally well predicted for the 4% slope. The two larger slopes generally have late predicted arrival times, especially for the off-axis sensors. In contrast to the continuous case, this result is consistent with the leading edge of the simulated current having a more pointed leading edge than in the experiment.

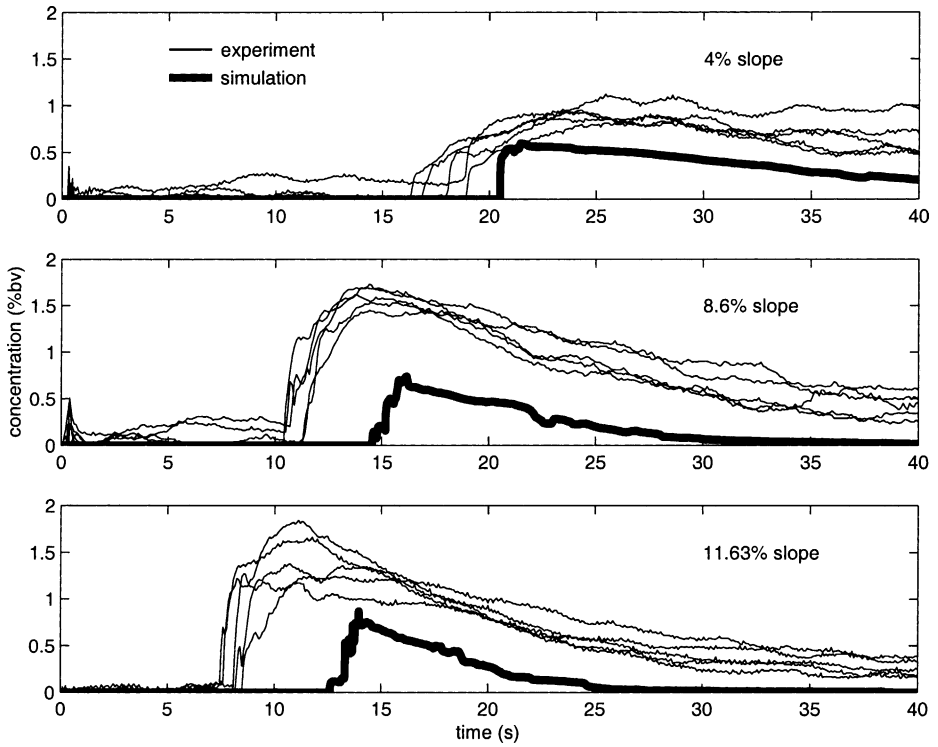

Fig. 2. Eulerian concentration traces at (184, 0) for each slope. From top to bottom: 4, 8.6, and 11.63%.

4.2. Physical assessment

A selection of TWODEE results is now chosen for more detailed examination, from a physical perspective. Eulerian concentration traces for two on-axis sensors is discussed, followed by a simulation snapshot taken 20 s after release.

4.2.1. Eulerian concentration traces

Figs. 1 and 2 show the concentration traces at (61, 0) and (184, 0), respectively; these sensors were chosen because they are the closest and furthest sensors on the centreline. The only difference between the three parts of each figure is the slope over which the gas was released. Several differences between the traces are apparent:

- The time of arrival decreases with increasing slope for the sensor at (184, 0); no trend is discernible at (61, 0). This would be expected with a fixed front Froude number as steeper slopes give taller leading edges and $u_f \propto h_f^{1/2}$.
- Peak concentration increases with increasing slope, although not significantly between the 8.6% slope and the 11.63% slope (either in the experiment or simulation). As discussed above, this is possibly connected to the narrower cloud width on steeper slopes.

- Residence time decreases with increasing slope. This would be expected as clouds on steeper slopes move faster.

These figures also show that cloud residence time is underpredicted. This is possibly due to the $(h/g')^{1/2}$ timescale resolution limit of shallow layer models. When the cloud becomes very dilute, this timescale becomes large and model predictions begin to degrade.

In each case, cloud residence time as defined in Section 3 is too small; the simulated cloud passes over the sensor too quickly. This is possibly due, as for the Thorney Island simulations, to the shallow water equations not being suitable for the early stages of an instantaneous release [4].

For the sensor at (61, 0), the model underpredicts peak concentrations on the 4% slope and the 11.63% slope, but is within the experimental bounds for the 8.6% slope. However, because the cloud residence time is too small in all three cases, the dose (defined as the integral of concentration with respect to time) is underpredicted by a factor of about two in each case. This is not to imply that there is a loss of dense material: the vertically integrated buoyancy flux past a point is proportional to layer depth and this quantity was not measured experimentally. In any case the TWODEE model is known to conserve buoyancy to better than one part in 10^4 [3]. Similar arguments apply to the sensor at (184,0).

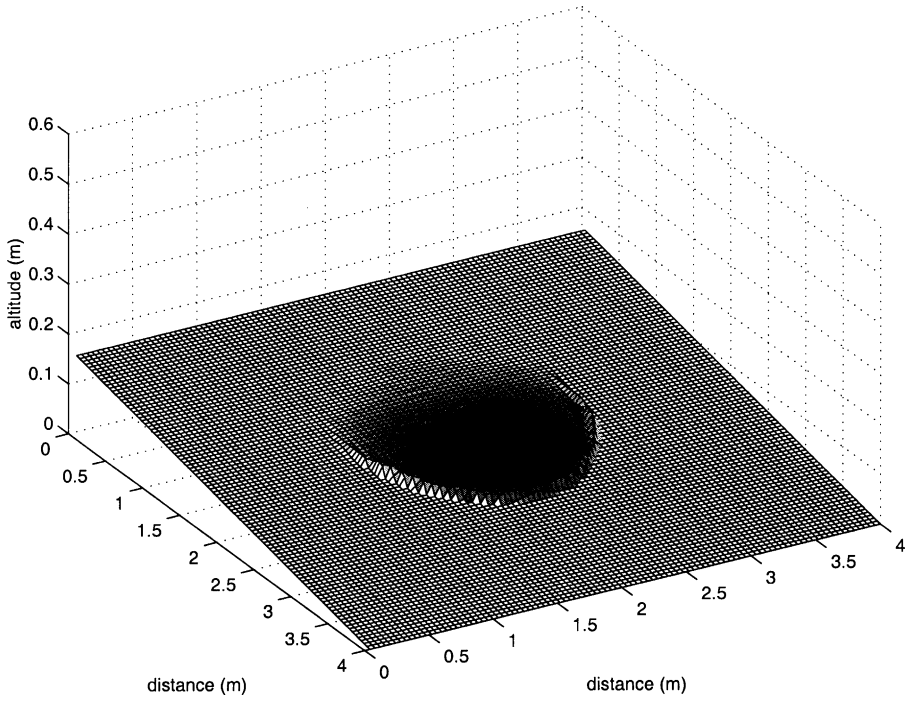

Fig. 3. Simulation for the 4% slope after 20 s; height of a point above the plane is the depth of the cloud. Shading of a point is proportional to the contaminant concentration. *Note*: Vertical scale differs from horizontal scales.

One interpretation of the underprediction seen in Figs. 1 and 2 is that the primary entrainment coefficient a [2] is too high. However, this should not be interpreted as a case for increasing a because most of the off-axis sensors were overpredicted (Table 2).

4.2.2. Perspective views of the simulation

Figs. 3–5 show, for the three slopes, the results of the simulation after 20 s. In each figure, the intensity of the plot shows the concentration, and the height of the plot is the depth of the dense layer. If the three simulations are compared and contrasted, common features include:

- In each case the leading edge is less dilute than the following flow; this is a consequence of edge entrainment being incompatible with a shallow layer approach [1,2].
- The leading edge is deeper than the following flow, as observed in one-dimensional gravity currents [23] on slopes in a calm ambient. However, although this resembles a gravity current head, it should be noted that shallow water simulations are capable of producing a head-like region near the leading edge as a result of a mismatch between the imposed boundary conditions and the following flow [24]. This detailed structure of the leading edge is not accessible to a shallow layer model, so the resemblance is fortuitous.
- The flows are superficially similar to the predictions of Webber et al. [24], Tickle [11], and Ross et al. [25] who all presented simple integral models of this situation.

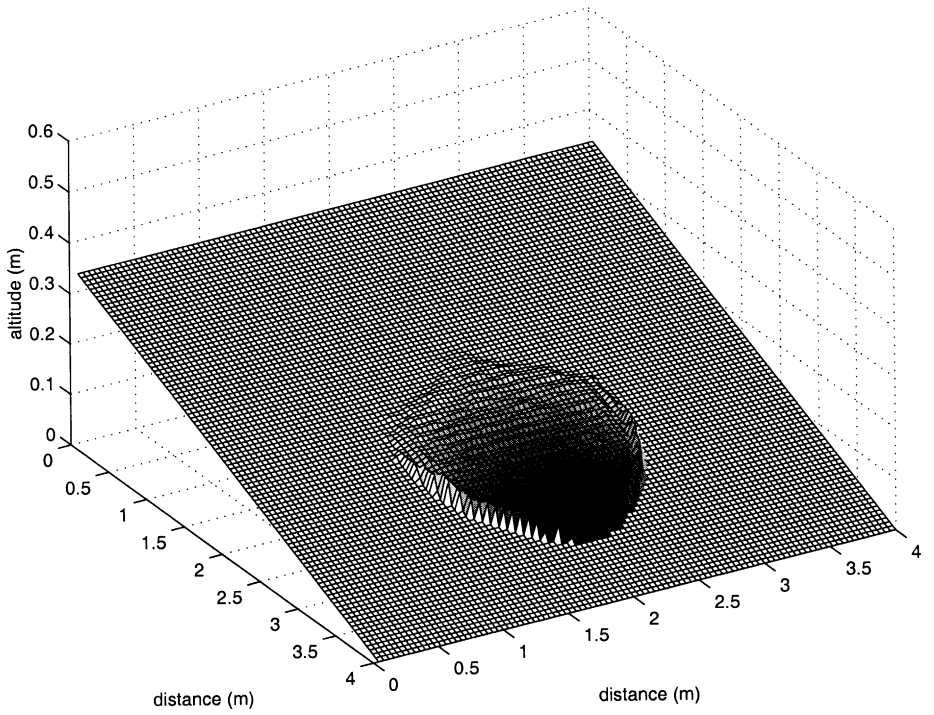

Fig. 4. Simulation for the 8.6% slope after 20 s; height of a point above the plane is the depth of the cloud. Shading of a point is proportional to the contaminant concentration. *Note*: Vertical scale differs from horizontal scales.

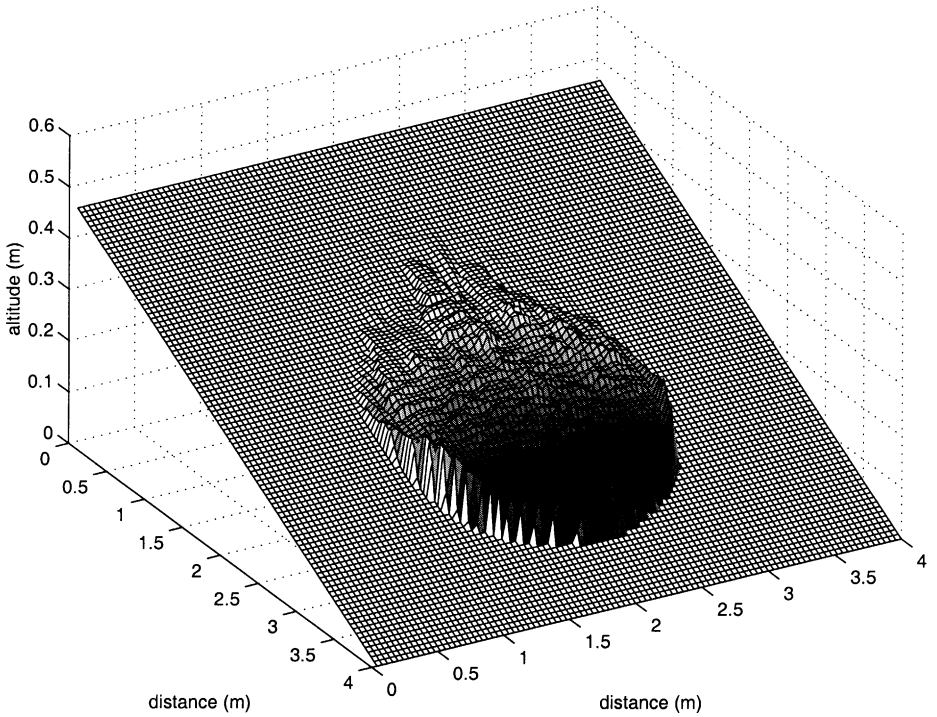

Fig. 5. Simulation for the 11.63% slope after 20 s; height of a point is the depth of the cloud Shading of a point is proportional to the contaminant concentration. *Note*: Vertical scale differs from horizontal scales.

However, this shallow layer model does reveal additional structure: the upper surface of the cloud is not horizontal, and density is not uniform over the cloud. Nevertheless, the similarity to all three models cited above is striking, even though the common finding of the cloud being wider than it is long does not have a unique analogue in the shallow water paradigm.

However, there are many features that differ between the slopes:

- The flow over steeper slopes is narrower. Cloud width rises from 2.1 m for the 4% slope through 2.3 m for 8.6%, to 2.6 m for 11.63%.
- The flow for the steeper slopes advanced further (at $t = 20$ s) than for the shallower slopes. This is consistent with the traces shown in Figs. 1 and 2 and shows that the flow travels faster over the steeper inclines. This is not observed in the one-dimensional experiments of Britter and Linden [23], so must be due to some aspect of the cross-slope flow.
- The flow over the shallower slopes is very much smoother (in terms of low cloud nonuniformity). Although this might be expected on physical grounds, it is not clear at this stage whether the simulation is reflecting a genuine physical process or is a numerical artifact.
- The region, behind the leading edge, of dilute flow is larger for the steeper slopes.

5. Summary

The shallow layer model TWODEE was used to simulate continuous and instantaneous releases over slopes in a calm ambient. The same model, with the same entrainment parameters, was used for both.

Predicted concentrations were generally underpredicted for the continuous releases, but were mostly correct to within a factor of two for the instantaneous releases.

A new system of assessment was presented that accounts for the repeated instantaneous releases; generalizations of MG and VG (viz. tG and FG) were presented. Both tG and FG were significantly larger than expected under the null hypothesis of homoscedastic, lognormally distributed observations with $\overline{\ln(C_{\mathrm{o},i})} = \ln(C_{\mathrm{p},i})$ for all sensors i.

The null hypothesis that the log of the mean residual was zero could be rejected for the 11.63% slope, but not the 4 or 8.6% slopes. However, these statistics were obtained in a calm ambient; their magnitude would be diminished outdoors by atmospheric variability.

For continuous releases, cloud arrival times were quite accurate for centreline sensors and late for off-axis sensors. Concentrations were generally correctly predicted to within a factor of two for the 4% slope, and to within a factor of about three for the other slopes.

For instantaneous releases arrival times tended to be late, especially for off-axis sensors. Cloud residence time was underpredicted for the instantaneous releases. Where predictions differed from experiment, physical explanations were given where possible.

This paper has shown that shallow layer models such as TWODEE can simulate the flows investigated by Schatzmann et al. [5] reasonably accurately, giving peak concentrations that are generally correct to within a factor of two.

References

[1] R.K.S. Hankin, Heavy gas dispersion over complex terrain, Ph.D. thesis, Cambridge University, 1997.
[2] R.K.S. Hankin, R.E. Britter, TWODEE: the health and safety laboratory's shallow layer model for dense gas dispersion. Part 1. Mathematical basis and physical assumptions, J. Hazard. Mater. 66 (3) (1999) 211–226.
[3] R.K.S. Hankin, R.E. Britter, TWODEE: the health and safety laboratory's shallow layer model for dense gas dispersion. Part 2. Outline and validation of the computational scheme, J. Hazard. Mater. 66 (3) (1999) 227–237.
[4] R.K.S. Hankin, R.E. Britter, TWODEE: the health and safety laboratory's shallow layer model for dense gas dispersion. Part 3. Experimental validation (Thorney Island), J. Hazard. Mater. 66 (3) (1999) 239–261.
[5] M. Schatzmann, K. Marotzke, J. Donat, Research on continuous and instantaneous heavy gas clouds, Contribution of sub-project EV 4T-0021-D to the final report of the joint CEC project, Technical report, Meteorological Institute, University of Hamburg, February 1991.
[6] S.R. Hanna, J.C. Chang, D.G. Strimaitis, Hazardous gas model evaluation with field observations, Atmos. Environ. 27A (15) (1993) 2265–2285.
[7] F.P. Lees, Loss Prevention in the Process Industries, vol. 1, second ed., Butterworth, Oxford, 2001.
[8] R.E. Britter, Atmospheric dispersion of dense gases, Annu. Rev. Fluid Mech. 21 (1989) 317–344.
[9] R.K.S. Hankin, Heavy gas dispersion: integral models and shallow layer models, J. Hazard. Mater. 103 (1–2) (2003) 1–10.
[10] J.E. Simpson, Gravity Currents in the Environment and the Laboratory, second ed., Cambridge University Press, Cambridge, 1997.
[11] G.A. Tickle, A model of the motion and dilution of a heavy gas cloud released on a uniform slope in calm conditions, J. Hazard. Mater. 49 (1996) 29–47.

[12] D.M. Webber, T. Wren, A differential phase equilibrium model for clouds, plumes and jets, Technical report SRD/HSE R552, AEA Technology, Consultancy Services, 1993.
[13] J. McQuaid, B. Roebuck, The dispersion of heavier-than-air gas from a fenced enclosure, Final report to the US Coast Guard on contract with the Health and Safety Executive, Technical report RPG 1185, Safety Engineering Laboratory, Research and Laboratory Services Division, Broad Lane, Sheffield, UK, 1985.
[14] M. Nielsen, S. Ott, A collection of data from dense gas experiments, Technical report Risø-R-845 (EN), Risø National Laboratory, Roskilde, Denmark, March 1996.
[15] M. Nielsen, Comment on 'A model of a heavy gas cloud released on a slope', J. Hazard. Mater. 48 (1996) 251–258.
[16] J.K.W. Davies, Discussion: hazardous gas model evaluation with field observations [6], Atmos. Environ. 29 (3) (1995) 455–458.
[17] A. Venkatram, Uncertainty in predictions from air quality models, Boundary Layer Meteorol. 27 (1983) 185–196.
[18] M.A. Fligner, T.J. Killeen, Distribution-free two-sample tests for scale, J. Am. Stat. Assoc. 71 (535) (1976) 210–213.
[19] W.J. Conover, M.E. Johnson, M.M. Johnson, A comparative study of tests for homogeneity of variances, with applications to the outer continental shelf-bidding data, Technometrics 23 (4) (1981) 351–361.
[20] A.W.F. Edwards, Likelihood, Johns Hopkins University Press, London, 1992.
[21] D.J. Wilson, Concentration Fluctuations and Averaging Time in Vapor Clouds, American Institute of Chemical Engineers, New York, 1995.
[22] T.H. Ellison, J.S. Turner, Turbulent entrainment in stratified flows, J. Fluid Mech. 6 (3) (1959) 529–544.
[23] R.E. Britter, P.F. Linden, The motion of the front of a gravity current travelling down an incline, J. Fluid Mech. 99 (3) (1980) 531–543.
[24] D.M. Webber, S.J. Jones, D. Martin, A model of the motion of a heavy gas cloud released on a uniform slope, J. Hazard. Mater. 33 (1993) 101–122.
[25] A. Ross, P.F. Linden, S.B. Dalziel, A study of three-dimensional gravity currents on a uniform slope, J. Fluid Mech. 453 (2002) 239–261.